Check for updates

# A highly active, thermally robust iron(III)/potassium(I) heterodinuclear catalyst for bio-derived epoxide/anhydride ring-opening copolymerizations†

Wilfred T. Diment, [ID] Gloria Rosetto, Noura Ezaz-Nikpay, Ryan W. F. Kerr [ID] and Charlotte K. Williams [ID] *

The ring-opening copolymerization (ROCOP) of epoxides and anhydrides is a useful route to polyesters but requires more active catalysts. An iron(III)/potassium(I) catalyst, applied without additives/co-catalyst, shows high rates, loading tolerance, thermal stability and selectivity. It shows unparalled rates using terpene-derived monomers, producing bio-derived, amorphous high glass transition temperature (>100 °C) polyesters relevant for future explorations as thermoplastics, block polymer adhesives and elastomers.

Polyesters are important as degradable, sustainable polymers which could contribute to a circular plastic economy. Many monomers are bio-derived, polymer properties are wide-ranging and, after use, many polyesters are recyclable: the ester linkages undergo chemical recycling and/or degradation.[1–3] Amorphous, high glass transition temperature ($T_g$ > 100 °C) bio-derived polyesters are particularly sought for use as thermoplastics and, within block polymer structures, as pressure sensitive adhesives or thermoplastic elastomers.[4–6] Here, epoxide/anhydride ring-opening copolymerization (ROCOP) furnishes such polyesters, applying both benchmark monomers (cyclohexene oxide (CHO) and phthalic anhydride (PA)) with bio-derived monomers.[4,7] The polymerizations are 100% atom economical, access different polymer structures and achieve high monomer conversions using functionalised and/or substituted monomers.[8,9]

This work focuses on catalyst development for cyclic, sterically hindered bio-derived monomers, a class of raw materials which limit polymer backbone segmental motion and produce amorphous polyesters showing high $T_g$ values.[10,11] In 2015 a ground-breaking report from Coates and co-workers described ROCOP-polyesters prepared from maleic anhydride and tri-

cyclic anhydrides from terpenes (α-terpinene and a-phellandrene).[12] Subsequently, other terpenes, *e.g.* limonene, menthene, eugenol, β-elemene, pinene, camphor and carene were transformed into monomers and ROCOP-polyesters.[7,13–18] Whilst the properties of terpene-derived polyesters are very interesting, these sterically hindered and rigid monomers retard polymerization rates. Thus, new catalysts combining high rates and selectivity are needed for these 'demanding' monomers.[7]

Generally, successful catalysts are benchmarked using CHO/PA ROCOP. High performance literature catalysts include complexes of Al(III),[19–21] Cr(III),[22,23] Y(III)[24] and Zn(II)[25] but many require PPNX co-catalysts which are expensive and may be toxic (where PPN = bis(triphenylphosphine)iminium, X = anion *e.g.* Cl⁻).[26] Recently, heterodinuclear catalysts operating without co-catalysts were reported.[27] For example, in 2021 an Al(III)/K(I) heterodinuclear catalyst showed a TOF of 1072 h⁻¹ (0.25 mol% *vs.* anhydride, 100 °C, CHO/PAO).[28] An Al(III)/K(I) organometallic catalyst yielded high molar mass polyesters (>90 kg mol⁻¹) with promise as engineering thermoplastics.[29] Here, an Fe(III)/K(I) complex, coordinated by the same ancillary ligand, is targeted (Fig. 1); the metal combination is selected based on catalytic precedent, elemental abundance, toxicity and cost.

Prior reports of s-block metal ROCOP catalysts, other than in the heterodinuclear catalyst above, include alkali–metal carboxylates/alkoxides. The most active, Cs(I) pivalate, showed moderate activity, with TOF ~40 h⁻¹ at high catalyst loading (2 mol% *vs.* anhydride, 100 °C, ethyl glycidyl ether/PA).[30–32] In the context of iron-containing complexes, Kleij and co-workers pioneered Fe(III)phenolate/PPNX catalyst systems but terpene-monomers showed lower rates (*e.g.* limonene oxide (LO)/PA; TOF = 8 h⁻¹, 0.5 mol%, 65 °C, toluene, Fig. S1, A†).[15,16,33] A dinuclear [Fe(III)]₂/2 PPNX catalyst system showed high activity, with TOF ~ 588 h⁻¹ (0.1 mol%, 100 °C, CHO/PA, Fig. S1, B†) but was not tested with terpene-derived monomers.[34] We reported an Fe(II)/Mg(II) catalyst for CHO/norbornene anhydride ROCOP, achieving a TOF of ~100 h⁻¹ (1 mol%, 100 °C).[35]

*Department of Chemistry, Chemistry Research Laboratory, University of Oxford, 12 Mansfield Road, Oxford, OX1 3TA, UK. E-mail: charlotte.williams@chem.ox.ac.uk*
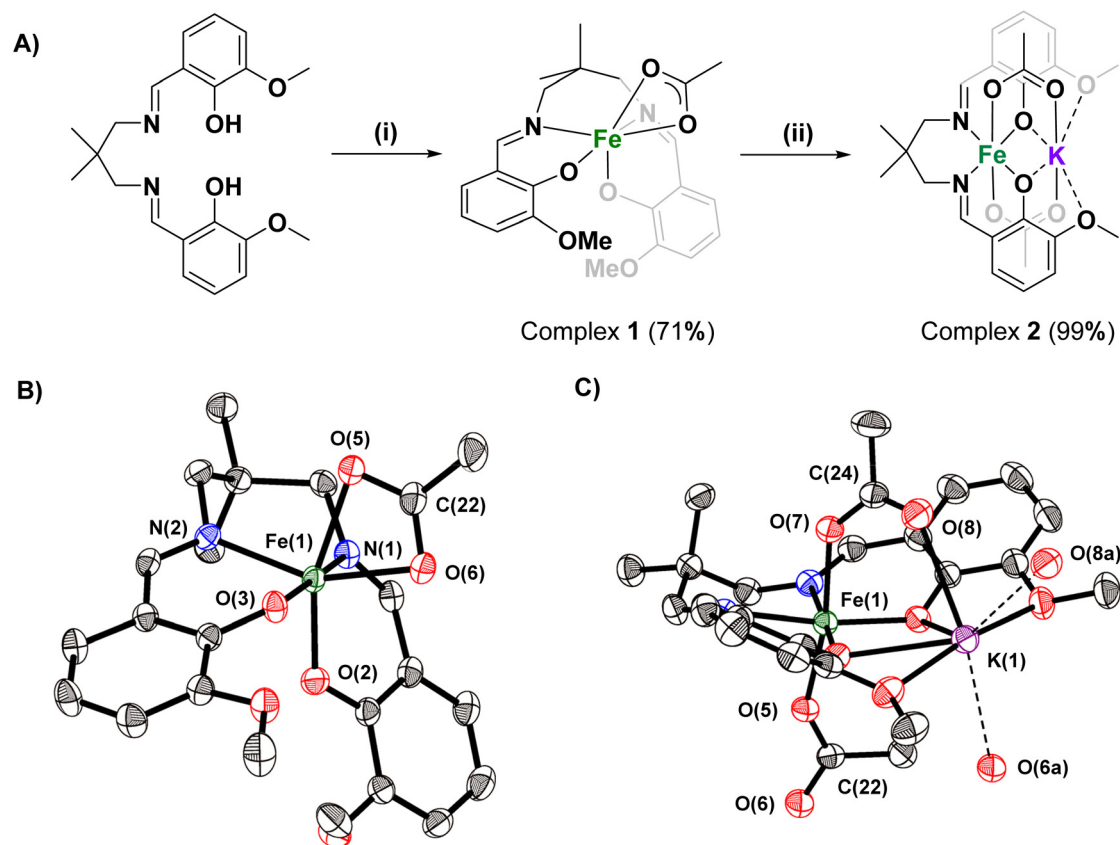
**Fig. 1** (A) Synthesis and characterisation of complexes **1** and **2**. (i) 1.0 equiv. Fe(OAc)$_2$, THF, 2 h, RT then air, 16 h, RT. (ii) 1.0 equiv. KOAc, 2-MeTHF, 16 h, RT. (B) Molecular structure of complex **1**, obtained from X-ray diffraction experiments. (C) Molecular structure of complex **2**, obtained from X-ray diffraction experiments. The structure is polymeric through O(8) and O(6); the monomeric unit is presented here for clarity. For both structures, thermal ellipsoids are presented at 50% probability and H-atoms are omitted for clarity. Selected bond lengths, angles, and crystallographic refinement data are presented in Tables S1–S3.†

The Fe(III)/K(I) heterodinuclear catalyst was synthesised *via* sequential metal addition since the ligand features coordination 'pockets' differentiating between transition metals (*O,N,N,O*-Schiff base moieties) and s-block metals (ether moieties), respectively.

The proligand, [L$_{van}$H$_2$], was reacted with an equivalent of Fe(II)(OAc)$_2$ to produce the Fe(II) complex, [L$_{van}$Fe], *in situ*. The complex was oxidized (in air) to form the new Fe(III) complex, [L$_{van}$FeOAc] (**1**), in good (70%) yield. Subsequent reaction of **1** with an equivalent of KOAc yielded the heterodinuclear complex [L$_{van}$FeK(OAc)$_2$] (**2**) in quantitative yield (Fig. 1A). The complexes were characterised using Super Conducting Quantum Interference Device (SQUID) magnetometry, IR spectroscopy and single crystal X-ray diffraction.

The molecular structure of complex **1** shows an octahedral Fe(III) centre, *cis*-β coordinated L$_{van}$, and a bidentate, κ$^2$-acetate group showing near-identical O(5/6)–C(22) bond lengths (Fig. 1B, Tables S1 and S2†).[36] The molecular structure of **2** confirms the heterodinuclear speciation with an octahedral Fe(III) and seven coordinate K(I). L$_{van}$ adopts an equatorial coordination mode around the Fe(III) center (Fig. 1C, Tables S1 and S3†). The two acetate ligands are both anionically coordinated

to the Fe(III) centre, *i.e.* a 'ferrate' structure, and both have different C–O bond lengths (*e.g.* C(24)–O(7) = 1.273(3) Å; C(24)–O(8) = 1.232(3) Å). The formation of the potassium ferrate complex is significant since it supports polymerization by the recently reported 'dinuclear metallate' mechanism.[27,28] To confirm that the solid-state molecular structures are consistent with the bulk material, IR spectroscopy and SQUID magnetometry were applied. SQUID magnetometry revealed a $\mu_{eff}$ of 6.10 and 5.69 for complexes **1** and **2** respectively, consistent with a single high spin, d$^5$, Fe(III) centre (Table S4 and Fig. S5†). The IR data support the formation of complexes **1** and **2**, with changes in the spectra supporting coordination of the potassium acetate, and corresponding shift of the acetate coordination mode (Fig. S2–S4†).

## Epoxide and Anhydride ROCOP catalysis

Complex **2** was tested as a catalyst for cyclohexene oxide (CHO) and phthalic anhydride (PA) ROCOP, at 100 °C, conditions that allow for benchmarking against literature catalysts. The cata-
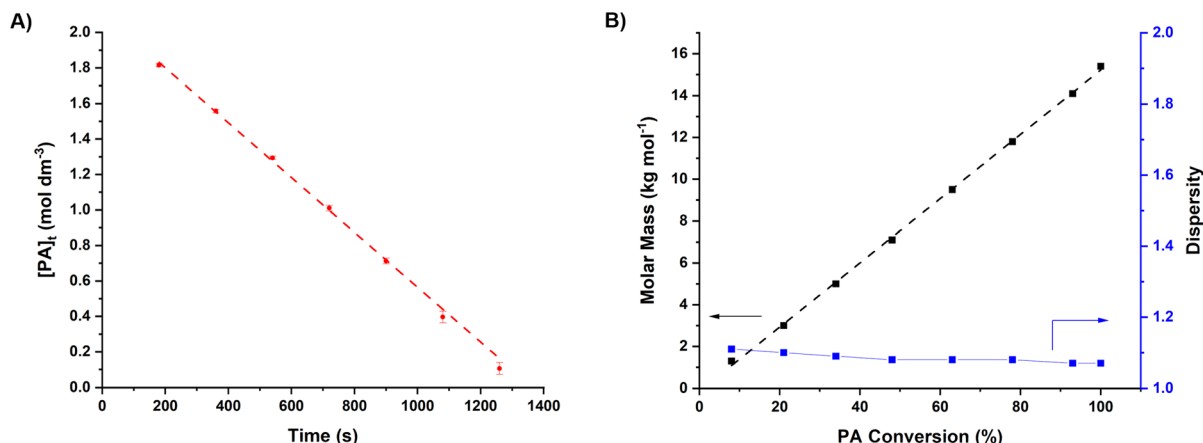
**Fig. 2** Catalyst benchmark data for the ROCOP of CHO and PA with complex **2**. Conditions: [**2**] : [PA] : [CHO] = 1 : 400 : 2000, $T$ = 100 °C. (A) Plot of [PA]$_t$ *vs.* time (s). Reaction displays a zero-order dependence on [PA]$_t$. Reactions repeated in triplicate, with average values of [PA]$_t$ plotted. (B) Plot of polymer molar mass, and dispersity, against PA conversion.

lyst showed exceptional activity, with a TOF of 1152 ± 20 h$^{-1}$ at low catalyst loading, 0.25 mol% catalyst *vs.* PA and 0.05 mol% catalyst *vs.* CHO. The catalyst also showed perfect selectivity (>99%) for polyester (PE) linkages (Fig. 2A, S6, S7† and Table 1, entry 2). Aliquot analysis showed a very short induction period (90 seconds) followed by fast, linear consumption of anhydride until complete monomer consumption.

The linear anhydride conversion *vs.* time data allowed for determination of the pseudo zero order rate coefficient, $k_{obs}$ = 1.55 ± 0.03 × 10$^{-3}$ mol dm$^{-3}$ s$^{-1}$, which is a high value under demanding conditions. The polymerization was well controlled showing a linear increase in polymer molar mass with monomer conversion producing polyesters with predictable molar mass values and low dispersity (Đ = 1.07) (Fig. 2B).

In comparison, the Fe(III) mononuclear complex **1** was very much less active, TOF = 72 h$^{-1}$, and showed reduced ester linkage selectivity, 73%, under identical conditions (Table 1, entry 1). It was previously reported that KOAc is a rather slow catalyst, even when applied at 4× higher loading (TOF = 23 h$^{-1}$,

1% *vs.* anhydride, $T$ = 110 °C).[31] These data highlight the importance of the heterodinuclear complexation in accelerating catalytic activity. Both the Fe(III) and K(I) centres are important, as is the ancillary ligand, in delivering the best performances.

In comparison to other CHO/PA ROCOP catalysts, complex **2** shows exceptional activity. Its rates are higher than any other heterodinuclear ROCOP catalyst reported so far, including the recently reported Al(III)/K(I) catalyst,[28] and amongst the highest in the field.[8,28] As mentioned in the introduction, there are few Fe(III) ROCOP catalysts but comparably, an Fe(III)(salen)(x) showed a low TOF of 3 h$^{-1}$ ($T$ = 100 °C, 1 mol% catalyst *vs.* PA, Fig. S1, C†).[37] The Fe(III)/K(I) catalyst, **2**, is 400× more active at one quarter of the loading. The dinuclear [LFe(III)$_2$]/PPNX catalyst system, under comparable conditions, showed a good activity, TOF = 588 h$^{-1}$ ($T$ = 100 °C, 0.1 mol% Fe center *vs.* PA, Fig. S1, B†); catalyst **2** shows 2× greater activity.[34] The Fe(III)(trisphenolate)(Cl)/PPNCl showed moderate activity but PA/CHO ROCOP was not reported preventing direct comparisons (Fig. S1, A†).[7]

**Table 1** Data for the ROCOP of CHO and PA using complex **2** under a range of conditions[a]

| Entry | Catalyst | [Cat] : [PA] | Temp (°C) | TON[b] | TOF[c] (h$^{-1}$) | PE select.[d] (%) | $M_{n,GPC}$[e] (kg mol$^{-1}$) | [Đ][f,g] |
|---|---|---|---|---|---|---|---|---|
| 1 | **1** | 400 | 100 | 144 ± 3 | 72 ± 2 | 73 | 7.5 | 1.15 |
| 2[g] | **2** | 400 | 100 | 288 ± 5 | 1152 ± 20 | >99 | 11.8 | 1.08 |
| 3[h] | **2** | 400 | 100 | 292 ± 5 | 1168 ± 20 | >99 | 9.0 | 1.12 |
| 4 | **2** | 400 | 120 | 312 ± 5 | 2340 ± 40 | >99 | 10.8 | 1.07 |
| 5 | **2** | 400 | 140 | 400 ± 7 | >4800 ± 82 | >99 | 14.0 | 1.08 |
| 6 | **2** | 1000 | 100 | 950 ± 16 | 950 ± 16 | >99 | 19.1 | 1.09 |
| 7 | **2** | 2000 | 100 | 1760 ± 30 | 880 ± 15 | >99 | 15.5 | 1.08 |
| 8 | **2** | 4000 | 100 | 3760 ± 63 | 627 ± 11 | 97 | 17.8 | 1.09 |
| 9 | **2** | 4000 | 140 | 3200 ± 54 | 3200 ± 54 | 96 | 14.1 | 1.08 |

[a] General conditions: [Cat] : [PA] : [CHO] = 1 : $x$ : $y$ where $x$ is given in table and $x$ : $y$ = 1 : 5 (*e.g* entry 1; [**2**] : [PA] : [CHO] = 1 : 400 : 2000). [b] Turnover number (TON) = number of moles of anhydride consumed/number of moles of catalyst. Calculated from PA conversion, see Table S5.† [c] Turnover frequency (TOF) = TON/time (hours). [d] Selectivity for polyester (PE) over polyether. Determined by $^1$H NMR spectrosocpy by comparison of integrals corresponding to PCHPE (5.22–5.06 ppm) and *poly*(CHO) (3.60–3.20 ppm). [e] Determined by gel permeation chromatography (GPC) in THF at 30 °C, using narrow dispersity polystyrene standards. Deviation from theoretical $M_n$ attributed to residual CTA present in polymerisation mixture, see Table S5 for details.† [f] Dispersity = $M_w/M_n$, determined by GPC in THF at 30 °C. [g] Time taken between 3 and 18 minutes to account for induction period observed. [h] Catalyst exposed to air for one week before reaction.

Next, the impacts of exposure of the catalyst to atmosphere, temperature and the influences of loading on catalytic activity were investigated (Table 1). It is particularly desirable to produce catalysts tolerant to low loadings and operable at high temperatures, the latter being an obvious way to accelerate rates using sterically hindered monomers.

Catalyst **2** is thermally robust maintaining high activity and polyester selectivity, at temperatures up to 140 °C (Table 1, entries 4 and 5). At 140 °C, it achieved an activity of 4800 h$^{-1}$ without any loss in selectivity – exceptional performance in this field. It also showed excellent air and moisture stability; exposing the catalyst to air for one week resulted in equivalent activity and selectivity, although molar mass values decreased consistent with water functioning as a chain transfer agent (Table 1, entry 3). The catalyst loading was also tested, although the benchmark conditions (1 : 400, 0.25 mol% *vs.* anhydride) are already lower than many tests conducted in this field.[28] The catalyst operated efficiently at 1 : 2000 (**2** : PA) and showed good rates and excellent selectivity (Table 1, entries 6 and 7). At very low catalyst loadings (1 : 4000, **2** : PA, 0.025 mol%), an activity of 700 h$^{-1}$ and 97% PE selectivity were obtained (Table 1, entry 8). Under these low loadings, increasing the temperature to 140 °C resulted in high activity, TOF = 3200 h$^{-1}$, whilst the PE selectivity was only slightly lower at 96% (Table 1, entry 9).

## Bio-derived monomers and polyesters

Catalyst **2** shows high rates in CHO/PA ROCOP and, therefore, was tested for demanding bio-derived epoxide/anhydride ROCOP (Fig. 3, Tables S6, S7 and Fig. S8–S12†). It is worth emphasis that routes to prepare CHO and PA from biomass have been reported.[38,39] Additionally, when targeting high $T_g$ polyesters, other bio-derived anhydrides, *e.g.* tricyclic anhydrides (TCA),[40] furan anhydride (FA),[41,42] and camphoric anhydride (CA),[43] are important targets (Fig. S13†). These monomers are targets for catalyst testing due to their tendency to enchain slowly as the steric hindrance reduces the accessibility of the carboxylate nucleophile.[44] Among bio-derived epoxides, limonene oxide (LO) and menthene oxide (MO)[45] should also form high $T_g$ polyesters and are derived directly from terpenes (Fig. S13†). Once again, they typically show low polymerization rates as they sterically inhibit carboxylate chain end attack.[15,45,46]

Complex **2** showed excellent activity and selectivity using all of these bio-derived monomers. High activities were obtained using TCA (TOF = 146 h$^{-1}$), CA (TOF = 106 h$^{-1}$) and FA (TOF = 148 h$^{-1}$), with perfect PE selectivity in all cases (Fig. 3 and Table S6, entries 1–3†). The catalyst also showed good activities for LO (TOF = 21 h$^{-1}$) and MO (TOF = 36 h$^{-1}$), again with no detectable ether formation (Fig. 1 and Table S6, entries 4 and 5†). It is faster than many literature catalysts tested with these monomers. For example, the Fe(III)(trisphenolate)/PPNCl showed a TCA/CHO ROCOP TOF = 15 h$^{-1}$ (0.33% *vs.* anhydride, 60 °C) and values of 8 h$^{-1}$ and 6 h$^{-1}$ for PA/LO and PA/MO, respectively (0.5% *vs.* anhydride, 65 °C).[15,16] Al(III)(salphen)(Cl)/PPNCl displayed an FA/CHO ROCOP TOF = 10 h$^{-1}$ (0.33% *vs.* FA, 60 °C).[10] An organocatalyst, $^t$BuP$_1$, displayed a PA/LO ROCOP TOF = 2 h$^{-1}$ (2% *vs.* anhydride, 100 °C).[13] Al(III)(salcy)(Cl)/PPNCl showed a CA/CHO ROCOP TOF = 2 h$^{-1}$ (70 °C, 1% *vs.* anhydride).[18] A Zn(II)Zn(II) catalyst gave a TCA/CHO ROCOP TOF = 11 h$^{-1}$ (100 °C, 1% *vs.* anhydride).[47] Overall, catalyst **2** showed 10–50× higher rates than leading literature catalysts highlighting its potential in bio-derived plastics production. To help inform future material
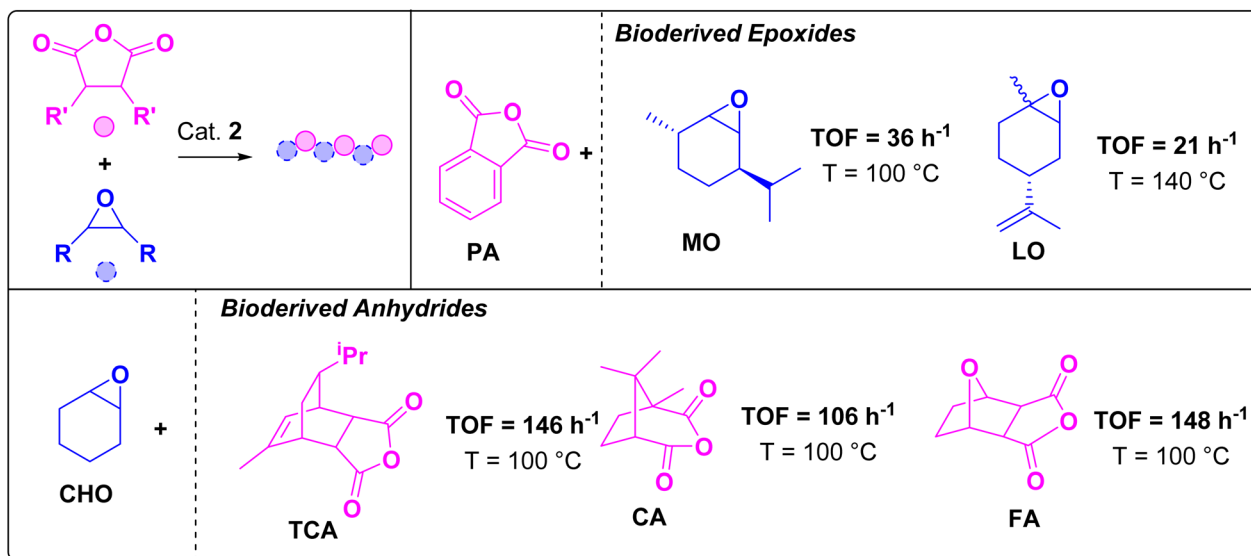


**Fig. 3** ROCOP of bio-derived epoxides and anhydrides. Polymerization conditions: [**2**] : [Anhydride] : [Epoxide] = 1 : 400 : 2000. PA/CHO held constant to allow for comparison of rates between monomer combinations. See Tables S6 and S7† for supporting data (including molar mass and dispersity).
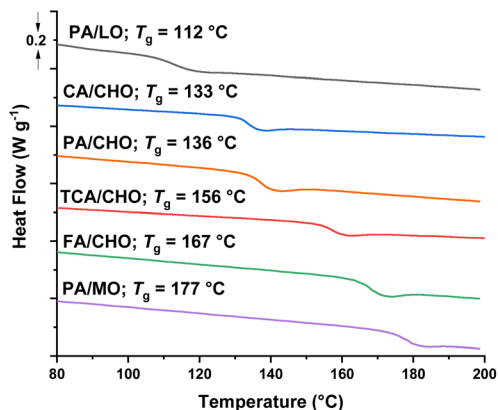
**Fig. 4** DSC Data for polyesters synthesised with bio-derived and epoxides. $T_g$ estimated from midpoint of transition during third heating curve.

development, all the polyesters were characterized *via* differential scanning calorimetry (DSC) and thermal gravimetric analysis (TGA) (Fig. 4, S15 and Table S7†). All polyesters were amorphous and showed the desired high glass transition temperatures ($T_g$), ranging from 112 (PA/LO) up to 177 °C (PA/MO). TGA analyses showed reasonable thermal stability and accessible processing temperature ranges. For example, the thermal decompositions temperatures ($T_{d,5\%}$) range from 253 °C (PA/LO) up to 360 °C (CHO/CA). The MO/PA polyester shows both a high $T_g$ (177 °C) and high $T_{d,5\%}$ 294 °C, making it a useful future candidate for rheological and mechanical testing.[15]

## Conclusions

The Fe(III)/K(I) heterodinuclear epoxide/anhydride ring-opening copolymerization catalyst showed high activity and selectivity using a range of monomers. The catalyst combined high rates (TOF = 1152 h$^{-1}$, 0.25 mol%, 100 °C), selectivity (>96%), thermal stability (100–140 °C) and loading tolerance (0.25–0.025 mol% *vs.* anhydride), as well as being air stable. The Fe(III)/K(I) complex outperforms analogous Fe(III) or K(I) complexes implicating heterodinuclear synergy (Fe(III)/K(I) = 16× faster than Fe(III) and 50× faster than K(I) analogues). The catalyst also showed field-leading activity and selectivity using challenging, sterically hindered terpene-derived monomers. It efficiently produced a series of amorphous, high $T_g$ (>100 °C) polyesters, which could be important in the future as thermoplastics, engineering polymers, resins and vitrimers.

The Fe(III)/K(I) combination should be tested using other ancillary ligands and as catalysts targeted for other polymerizations, *e.g.* carbon dioxide/epoxide ROCOP or lactide, lactone or cyclic carbonate ring-opening polymerizations which may benefit from heterodinuclear synergy,[48–50] and where iron-containing catalysts have been shown to be effective.[51–53] In order to target high molar mass polyesters, an organometallic derivative of the Fe(III)/K(I) catalyst should also be targeted.[29]

## Author contributions

Experimental procedures carried out by WD, GR and NE-N. CW and WD wrote the manuscript.

## Conflicts of interest

There are no conflicts to declare.

## Acknowledgements

## References

1 R. M. Cywar, N. A. Rorrer, C. B. Hoyt, G. T. Beckham and E. Y. X. Chen, *Nat. Rev. Mater.*, 2022, **7**, 83–103.
2 J. Payne and M. D. Jones, *ChemSusChem*, 2021, **14**, 4041–4070.
3 M. A. Hillmyer, *Science*, 2017, **358**, 868–870.
4 T. T. D. Chen, L. P. Carrodeguas, G. S. Sulley, G. L. Gregory and C. K. Williams, *Angew. Chem., Int. Ed.*, 2020, **59**, 23450–23455.
5 F. Della Monica and A. W. Kleij, *Polym. Chem.*, 2020, **11**, 5109–5127.
6 T. M. McGuire, E. F. Clark and A. Buchard, *Macromolecules*, 2021, **54**, 5094–5105.
7 A. Brandolese and A. W. Kleij, *Acc. Chem. Res.*, 2022, **55**, 1634–1645.
8 S. Paul, Y. Q. Zhu, C. Romain, R. Brooks, P. K. Saini and C. K. Williams, *Chem. Commun.*, 2015, **51**, 6459–6479.
9 J. M. Longo, M. J. Sanford and G. W. Coates, *Chem. Rev.*, 2016, **116**, 15167–15197.
10 X. Yu, J. Jia, S. Xu, K. U. Lao, M. J. Sanford, R. K. Ramakrishnan, S. I. Nazarenko, T. R. Hoye, G. W. Coates and R. A. DiStasio Jr., *Nat. Commun.*, 2018, **9**, 2880.
11 M. Winkler, C. Romain, M. A. R. Meier and C. K. Williams, *Green Chem.*, 2015, **17**, 300–306.
12 N. J. Van Zee and G. W. Coates, *Angew. Chem. Int. Ed.*, 2015, **54**, 2665–2668.
13 H. Li, H. T. Luo, J. P. Zhao and G. Z. Zhang, *Macromolecules*, 2018, **51**, 2247–2257.
14 F. D. Monica and A. W. Kleij, *ACS Sustainable Chem. Eng.*, 2021, **9**, 2619–2625.
15 L. Peña Carrodeguas, C. Martín and A. W. Kleij, *Macromolecules*, 2017, **50**, 5337–5345.
16 M. J. Sanford, L. Peña Carrodeguas, N. J. Van Zee, A. W. Kleij and G. W. Coates, *Macromolecules*, 2016, **49**, 6394–6400.

17 B. Liu, J. Chen, N. Liu, H. Ding, X. Wu, B. Dai and I. Kim, *Green Chem.*, 2020, **22**, 5742–5750.

18 C. Robert, F. de Montigny and C. M. Thomas, *Nat. Commun.*, 2011, **2**, 586.

19 B. A. Abel, C. A. L. Lidston and G. W. Coates, *J. Am. Chem. Soc.*, 2019, **141**, 12760–12769.

20 J. Li, Y. Liu, W.-M. Ren and X.-B. Lu, *J. Am. Chem. Soc.*, 2016, **138**, 11493–11496.

21 Y. N. Li, Y. Liu, H. H. Yang, W. F. Zhang and X. B. Lu, *Angew. Chem., Int. Ed.*, 2022, **61**, e202202585.

22 L. Cui, B. H. Ren and X. B. Lu, *J. Polym. Sci.*, 2021, **59**, 1821–1828.

23 E. Hosseini Nejad, C. G. W. van Melis, T. J. Vermeer, C. E. Koning and R. Duchateau, *Macromolecules*, 2012, **45**, 1770–1776.

24 Y. Manjarrez, M. D. C. L. Cheng-Tan and M. E. Fieser, *Inorg. Chem.*, 2022, **61**, 7088–7094.

25 R. C. Jeske, A. M. DiCiccio and G. W. Coates, *J. Am. Chem. Soc.*, 2007, **129**, 11330–11331.

26 C. A. L. Lidston, S. M. Severson, B. A. Abel and G. W. Coates, *ACS Catal.*, 2022, **12**, 11037–11070.

27 W. T. Diment, W. Lindeboom, F. Fiorentini, A. C. Deacy and C. K. Williams, *Acc. Chem. Res.*, 2022, **55**(15), 1997–2010.

28 W. T. Diment, G. L. Gregory, R. W. F. Kerr, A. Phanopoulos, A. Buchard and C. K. Williams, *ACS Catal.*, 2021, **11**, 12532–12542.

29 W. T. Diment and C. K. Williams, *Chem. Sci.*, 2022, **13**, 8543–8549.

30 X. Xia, R. Suzuki, K. Takojima, D. Jiang, T. Isono and T. Satoh, *ACS Catal.*, 2021, **11**, 5999–6009.

31 C.-M. Chen, X. Xu, H.-Y. Ji, B. Wang, L. Pan, Y. Luo and Y.-S. Li, *Macromolecules*, 2021, **54**, 713–724.

32 X. Xia, R. Suzuki, T. Gao, T. Isono and T. Satoh, *Nat. Commun.*, 2022, **13**, 163.

33 M. Taherimehr, S. M. Al-Amsyar, C. J. Whiteoak, A. W. Kleij and P. P. Pescarmona, *Green Chem.*, 2013, **15**, 3083–3090.

34 Z. Shi, Q. Z. Jiang, Z. Z. Song, Z. H. Wang and C. L. Gao, *Polym. Chem.*, 2018, **9**, 4733–4743.

35 N. V. Reis, A. C. Deacy, G. Rosetto, C. B. Durr and C. K. Williams, *Chem. – Eur. J.*, 2022, **28**, e202104198.

36 W. T. Diment, T. Stosser, R. W. F. Kerr, A. Phanopoulos, C. B. Durr and C. K. Williams, *Catal. Sci. Technol.*, 2021, **11**, 1737–1745.

37 O. J. Driscoll, J. A. Stewart, P. McKeown and M. D. Jones, *Macromolecules*, 2021, **54**, 8443–8452.

38 S. Giarola, C. Romain, C. K. Williams, J. P. Hallett and N. Shah, *Chem. Eng. Res. Des.*, 2016, **107**, 181–194.

39 E. Mahmoud, D. A. Watson and R. F. Lobo, *Green Chem.*, 2014, **16**, 167–175.

40 D. Dakshinamoorthy, A. K. Weinstock, K. Damodaran, D. F. Iwig and R. T. Mathers, *ChemSusChem*, 2014, **7**, 2923–2929.

41 A. E. Settle, L. Berstis, N. A. Rorrer, Y. Roman-Leshkóv, G. T. Beckham, R. M. Richards and D. R. Vardon, *Green Chem.*, 2017, **19**, 3468–3492.

42 S. Thiyagarajan, H. C. Genuino, M. Śliwa, J. C. van der Waal, E. de Jong, J. van Haveren, B. M. Weckhuysen, P. C. A. Bruijnincx and D. S. van Es, *ChemSusChem*, 2015, **8**, 3052–3056.

43 M. G. Moloney, D. R. Paul, R. M. Thompson and E. Wright, *Tetrahedron: Asymmetry*, 1996, **7**, 2551–2562.

44 H. Zhang, J. Li, Z. Tian and F. Liu, *J. Appl. Polym. Sci.*, 2013, **129**, 3333–3340.

45 A. Wambach, S. Agarwal and A. Greiner, *ACS Sustainable Chem. Eng.*, 2020, **8**, 14690–14693.

46 J. A. Mmongoyo, Q. A. Mgani, S. J. M. Mdachi, P. J. Pogorzelec and D. J. Cole-Hamilton, *Eur. J. Lipid Sci. Technol.*, 2012, **114**, 1183–1192.

47 G. Rosetto, A. C. Deacy and C. K. Williams, *Chem. Sci.*, 2021, **12**, 12315–12325.

48 W. Gruszka and J. A. Garden, *Nat. Commun.*, 2021, **12**, 3252.

49 Y. Zhou, G. S. Nichol and J. A. Garden, *Eur. J. Inorg. Chem.*, 2022, **2022**, e202200134.

50 W. Gruszka and J. A. Garden, *Chem. Commun.*, 2022, **58**, 1609–1612.

51 M. Qi, Q. Dong, D. Wang and J. A. Byers, *J. Am. Chem. Soc.*, 2018, **140**, 5686–5690.

52 A. B. Biernesser, K. R. Delle Chiaie, J. B. Curley and J. A. Byers, *Angew. Chem., Int. Ed.*, 2016, **55**, 5251–5254.

53 A. B. Biernesser, B. Li and J. A. Byers, *J. Am. Chem. Soc.*, 2013, **135**, 16553–16560.